

Generalized kinetic model for defect evolution in irradiated materials

Galen T. Craven*

Theoretical Division, Los Alamos National Laboratory, Los Alamos, New Mexico 87544

Brandon M. Wilson†

*X Computational Physics Division, Los Alamos
National Laboratory, Los Alamos, New Mexico 87544*

A fundamental and open problem in materials science is to determine how the structural properties of irradiated and self-irradiated materials evolve in time. Structural defects generated by irradiation lead to changes in a material’s macroscopic properties, and these macroscopic changes, such as volumetric swelling, can in turn give rise significant alterations of the functionality of a material. Here, we develop a unified analytical model to understand the complex interplay between aggregation, fragmentation, and recombination processes involving mobile clusters of defects such as bubbles, voids, and interstitial atoms in materials subject to radiative sources. Specifically, we employ a mean field approach to derive a system of coupled kinetic equations that describes both the time evolution of the density of each type of defect and how clusters of each defect form and grow as the material ages.

I. INTRODUCTION

Understanding how irradiation and self-irradiation processes affect the structural properties of materials, and how in turn these altered structural properties give rise to changes in a material’s functionality has generated substantial interest due to it’s importance for a number of security, energy, and industrial applications.¹⁻⁶ Elucidating and predicting these processes is particularly important both in nuclear materials and in other materials that are used in the construction of nuclear reactors. Theoretical and computational work plays a prominent role in studies that seek to understand and predict the outcome of these processes because (a) experimental measurements are often not available due to security and safety protocols that make performing measurements on nuclear materials difficult without specific

infrastructure and (b) the experimental timescales—often of the order tens of years—that are needed to evolve these materials into states of interest.⁷ In some cases artificial irradiation can be used to mimic and accelerate the aging process of nuclear materials, but artificial aging often does not result in the same altered structures that arise from natural aging and therefore provides only a qualitative picture of a material’s natural time evolution. Because obtaining experimental measurements is cumbersome, developing theoretical models that quantitatively capture the effects of irradiation is of paramount importance in the fields of theoretical and computational materials science. Some of the primary goals of these studies are to enhance the safety and assess the function of aging nuclear materials.

Previous theoretical work on the kinetics of irradiated materials has focused on the development of systems of master equations that describe how clusters of point defects evolve in time.^{5,8–10} The defect type, or combination of defect types, that dominate the structural changes generated by irradiation is often specific to the material. In general, some combination of bubbles (clusters of gas atoms that are generated by nuclear processes), voids (clusters of vacancies), interstitial clusters, and bubble-void clusters are present after irradiation.^{5,9,11–13} Interstitial-void clusters are typically not observed due to the propensity of these two defects to combine. Additionally, the propensity of bubbles and interstitial clusters to aggregate depends significantly on the material, and, in general, the propensity of each defect type to cluster with itself and with other defect types is material dependent.^{11,12,14–24}

One of the core approaches used to understand and predict defect evolution in materials is cluster dynamics.^{3–6,8,9,25} Cluster dynamics models can be used to predict complex coupling and interplay between aggregating defect types, the mobility of defects, and the fragmentation of clusters. In a cluster dynamics simulation, a mean-field method is used to track the time evolution of concentrations or densities of point defects and defect clusters.^{6,23,24}

Here, we develop a dynamical system based on cluster dynamics that describes point defect evolution and the growth of defect clusters in irradiated materials.^{4,17,20} The developed model incorporates aggregation, fragmentation, recombination processes while accounting for the mobility of defect clusters of various sizes. More specifically, a mean field theory is used to derive a system of coupled kinetic equations that describes the time evolution of the density of bubbles, voids, bubble-void clusters, and clusters of interstitial atoms. The rate constants in the model are derived using the Arrhenius kinetic picture and ideas adopted from other rate theories including transition state theory²⁶ and classical nucleation theory.²⁷

The rest of the report is organized as follows: Section II contains the details of kinetic scheme we use to model defect and cluster growth in irradiated and self-irradiated materials. The details of the rate constants that are used in this model are presented in Sec. III. Concluding remarks are presented in Sec. IV.

II. MODEL

The dynamical system we employ to model defect cluster and void evolution in irradiated materials is defined by the coupled set of kinetic equations:

$$\begin{aligned} \dot{\rho}_1^{(b)} = & G_b(t) - \sum_{i=1}^{\infty} (1 + \delta_{i,1}) A_{i,1}^{(b)} \rho_i^{(b)} \rho_1^{(b)} - \sum_{i=1}^{\infty} A_{i,1}^{(v,b)} \rho_i^{(v)} \rho_1^{(b)} - \sum_{i=1}^{\infty} \sum_{j=1}^{\infty} A_{\{i,j\},1}^{(bv,b)} \rho_{\{i,j\}}^{(bv)} \rho_1^{(b)} \\ & + \sum_{i=2}^{\infty} (1 + \delta_{i-1,1}) F_{i \rightarrow i-1,1}^{(b)} \rho_i^{(b)} + \sum_{i=1}^{\infty} \sum_{j=1}^{\infty} F_{\{i,j\} \rightarrow \{1,0\}, \{i-1,j\}}^{(bv)} \rho_{i,j}^{(bv)}, \end{aligned} \quad (1)$$

$$\begin{aligned} \dot{\rho}_k^{(b)} = & - \sum_{i=1}^{\infty} (1 + \delta_{i,k}) A_{i,k}^{(b)} \rho_i^{(b)} \rho_k^{(b)} - \sum_{i=1}^{\infty} A_{i,k}^{(v,b)} \rho_i^{(v)} \rho_k^{(b)} - \sum_{i=1}^{\infty} \sum_{j=1}^{\infty} A_{\{i,j\},k}^{(bv,b)} \rho_{\{i,j\}}^{(bv)} \rho_k^{(b)} \\ & + \frac{1}{2} \sum_{i=1}^{k-1} (1 + \delta_{i,k-i}) A_{i,k-i}^{(b)} \rho_i^{(b)} \rho_{k-i}^{(b)} - \frac{1}{2} \sum_{i=1}^{k-1} (1 + \delta_{i,k-i}) F_{k \rightarrow i,k-i}^{(b)} \rho_k^{(b)} \\ & + \sum_{i=k+1}^{\infty} (1 + \delta_{i-k,k}) F_{i \rightarrow i-k,k}^{(b)} \rho_i^{(b)} + \sum_{i=k}^{\infty} \sum_{j=1}^{\infty} F_{\{i,j\} \rightarrow \{i-k,j\}, \{k,0\}}^{(bv)} \rho_{i,j}^{(bv)}, \end{aligned} \quad (2)$$

$$\begin{aligned} \dot{\rho}_1^{(v)} = & G_v(t) - \sum_{i=1}^{\infty} (1 + \delta_{i,1}) A_{i,1}^{(v)} \rho_i^{(v)} \rho_1^{(v)} - \sum_{i=1}^{\infty} A_{1,i}^{(v,b)} \rho_1^{(v)} \rho_i^{(b)} - \sum_{i=1}^{\infty} \sum_{j=1}^{\infty} A_{\{i,j\},1}^{(bv,v)} \rho_{\{i,j\}}^{(bv)} \rho_1^{(v)} \\ & + \sum_{i=2}^{\infty} (1 + \delta_{i-1,1}) F_{i \rightarrow i-1,1}^{(b)} \rho_i^{(v)} + \sum_{i=1}^{\infty} \sum_{j=1}^{\infty} F_{\{i,j\} \rightarrow \{0,1\}, \{i,j-1\}}^{(bv)} \rho_{i,j}^{(bv)} \\ & - \sum_{i=1}^{\infty} R_{1,i}^{(v,int)} \rho_1^{(v)} \rho_i^{(int)} + \sum_{i=2}^{\infty} \sum_{j=i-1}^{\infty} R_{i,j}^{(v,int)} \rho_i^{(v)} \rho_j^{(int)}, \end{aligned} \quad (3)$$

$$\begin{aligned} \dot{\rho}_k^{(v)} = & - \sum_{i=1}^{\infty} (1 + \delta_{i,k}) A_{i,k}^{(v)} \rho_i^{(v)} \rho_k^{(v)} - \sum_{i=1}^{\infty} A_{k,i}^{(v,b)} \rho_k^{(v)} \rho_i^{(b)} - \sum_{i=1}^{\infty} \sum_{j=1}^{\infty} A_{\{i,j\},k}^{(bv,v)} \rho_{\{i,j\}}^{(bv)} \rho_k^{(v)} \\ & + \frac{1}{2} \sum_{i=1}^{k-1} (1 + \delta_{i,k-i}) A_{i,k-i}^{(v)} \rho_i^{(v)} \rho_{k-i}^{(v)} - \frac{1}{2} \sum_{i=1}^{k-1} (1 + \delta_{i,k-i}) F_{k \rightarrow i,k-i}^{(v)} \rho_k^{(v)} \\ & + \sum_{i=k+1}^{\infty} (1 + \delta_{i-k,k}) F_{i \rightarrow i-k,k}^{(v)} \rho_i^{(v)} + \sum_{i=1}^{\infty} \sum_{j=k}^{\infty} F_{\{i,j\} \rightarrow \{i,j-k\}, \{0,k\}}^{(bv)} \rho_{i,j}^{(bv)} \end{aligned}$$

$$- \sum_{i=1}^{\infty} R_{k,i}^{(v,\text{int})} \rho_k^{(v)} \rho_i^{(\text{int})} + \sum_{i=k+1}^{\infty} \sum_{j=i-1}^{\infty} R_{j,i}^{(v,\text{int})} \rho_i^{(v)} \rho_j^{(\text{int})}, \quad (4)$$

$$\begin{aligned} \dot{\rho}_{\{k,l\}}^{(bv)} = & - \sum_{i=1}^{\infty} A_{\{k,l\},i}^{(bv,b)} \rho_{\{k,l\}}^{(bv)} \rho_i^{(b)} - \sum_{i=1}^{\infty} A_{\{k,l\},i}^{(bv,v)} \rho_{\{k,l\}}^{(bv)} \rho_i^{(v)} \\ & - \sum_{i=1}^{\infty} \sum_{j=1}^{\infty} (1 + \delta_{\{k,l\},\{i,j\}}) A_{\{k,l\},\{i,j\}}^{(bv)} \rho_{\{k,l\}}^{(bv)} \rho_{\{i,j\}}^{(bv)} + \sum_{i=1}^{k-1} A_{\{k-i,l\},i}^{(bv,b)} \rho_{\{k-i,l\}}^{(bv)} \rho_i^{(b)} \\ & + \sum_{i=1}^{l-1} A_{\{k,l-i\},i}^{(bv,v)} \rho_{\{k,l-i\}}^{(bv)} \rho_i^{(v)} + A_{k,l}^{(b,v)} \rho_k^{(b)} \rho_l^{(v)} + \sum_{i=1}^{k-1} \sum_{j=1}^{l-1} A_{\{k-i,l-j\},\{i,j\}}^{(bv)} \rho_{\{k-i,l-j\}}^{(bv)} \rho_{\{i,j\}}^{(bv)} \\ & - \sum_{i=1}^k \left(1 - \frac{\delta_{k-i,0}}{2}\right) F_{\{k,l\} \rightarrow \{k-i,l\},\{i,0\}}^{(bv)} \rho_{\{k,l\}}^{(bv)} - \sum_{i=1}^l \left(1 - \frac{\delta_{l-i,0}}{2}\right) F_{\{k,l\} \rightarrow \{k,l-i\},\{0,i\}}^{(bv)} \rho_{\{k,l\}}^{(bv)} \\ & - \sum_{i=1}^{k-1} \sum_{j=1}^{l-1} F_{\{k,l\} \rightarrow \{k-i,l-j\},\{i,j\}}^{(bv)} \rho_{\{k,l\}}^{(bv)} + \sum_{i=1}^{\infty} F_{\{k+i,l\} \rightarrow \{k,l\},\{i,0\}}^{(bv)} \rho_{\{k+i,l\}}^{(bv)} \\ & + \sum_{i=1}^{\infty} F_{\{k,l+i\} \rightarrow \{k,l\},\{0,i\}}^{(bv)} \rho_{\{k,l+i\}}^{(bv)} + \sum_{i=1}^{\infty} \sum_{j=1}^{\infty} F_{\{k+i,l+j\} \rightarrow \{k,l\},\{i,j\}}^{(bv)} \rho_{\{k+i,l+j\}}^{(bv)}, \end{aligned} \quad (5)$$

$$\begin{aligned} \dot{\rho}_1^{(\text{int})} = & G_{\text{int}}(t) - \sum_{i=1}^{\infty} (1 + \delta_{i,1}) A_{i,1}^{(\text{int})} \rho_i^{(\text{int})} \rho_1^{(\text{int})} + \sum_{i=2}^{\infty} (1 + \delta_{i-1,1}) F_{i \rightarrow i-1,1}^{(\text{int})} \rho_i^{(\text{int})} \\ & - \sum_{i=1}^{\infty} R_{i,1}^{(v,\text{int})} \rho_i^{(v)} \rho_1^{(\text{int})} + \sum_{i=2}^{\infty} \sum_{j=i-1}^{\infty} R_{j,i}^{(v,\text{int})} \rho_j^{(v)} \rho_i^{(\text{int})}, \end{aligned} \quad (6)$$

$$\begin{aligned} \dot{\rho}_k^{(\text{int})} = & - \sum_{i=1}^{\infty} (1 + \delta_{i,k}) A_{i,k}^{(\text{int})} \rho_i^{(\text{int})} \rho_k^{(\text{int})} + \frac{1}{2} \sum_{i=1}^{k-1} (1 + \delta_{i,k-i}) A_{i,k-i}^{(\text{int})} \rho_i^{(\text{int})} \rho_{k-i}^{(\text{int})} \\ & - \frac{1}{2} \sum_{i=1}^{k-1} (1 + \delta_{k-i,i}) F_{k \rightarrow k-i,i}^{(\text{int})} \rho_k^{(\text{int})} + \sum_{i=k+1}^{\infty} (1 + \delta_{i-k,k}) F_{i \rightarrow i-k,k}^{(\text{int})} \rho_i^{(\text{int})} \\ & - \sum_{i=1}^{\infty} R_{i,k}^{(v,\text{int})} \rho_i^{(v)} \rho_k^{(\text{int})} + \sum_{i=k+1}^{\infty} \sum_{j=i-1}^{\infty} R_{j,i}^{(v,\text{int})} \rho_j^{(v)} \rho_i^{(\text{int})}, \end{aligned} \quad (7)$$

where $\rho_k^{(b)}$ is the density of bubbles consisting of k atoms (k -bubbles), $\rho_{k,l}^{(bv)}$ is the density of bubble-void clusters consisting of k atoms and l vacancies ($\{k,l\}$ -bubbles), $\rho_k^{(v)}$ is the density of voids consisting of k vacancies (k -voids), and $\rho_k^{(\text{int})}$ is the density of clusters of interstitial atoms consisting of k atoms (k -clusters). The prefactors A , F , and R are respectively *aggregation*, *fragmentation*, and *recombination* rate constants for the different reactions where the species involved in each specific reaction is given in the superscript. The subscript in each aggregation and recombination rate constant indicates the size of the two bubbles, bubble-void clusters, voids, and/or interstitial clusters that are reacting.

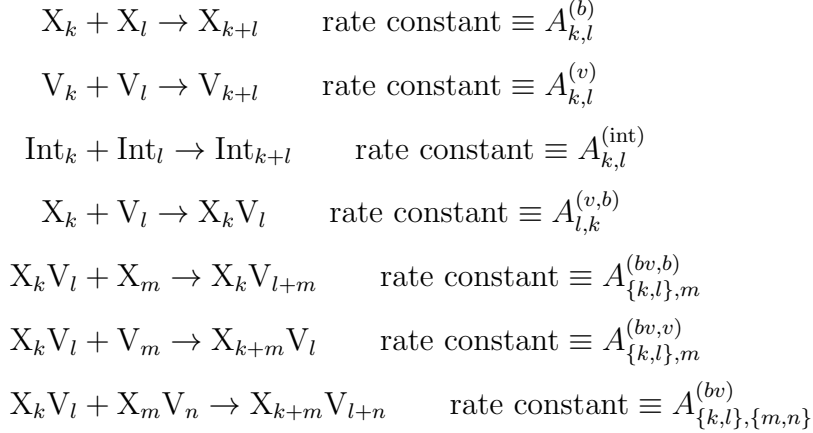
Here, the only type of fragmentation processes considered are reactions that result in two fragments. The fragmentation rate constant subscripts indicate the size of the initial cluster and the size of the two product fragments. More detail about the rate constants is given in Sec. III. The symbol $\delta_{i,j}$ is the Kronecker delta. The terms $G_b(t)$ and $G_v(t)$ are the *generation* rates for monomeric gas (1-bubbles) and vacancies (1-voids), respectively. The generation rate of interstitial atoms (1-clusters), $G_{\text{int}}(t)$, is equal to the generation rate of vacancies. Generation rate terms for defects of size > 1 can be easily added to the model if needed.

We ignore the spatial dependence of each density term by assuming that defect generation takes place uniformly through the material and that defect migration is an isotropic process. Interstitial-gas aggregation terms are not included in the model because it has been observed in multiple systems that these clusters are not stable due to strong repulsion between interstitial atoms and gas atoms. Sink terms are also excluded so as focus on the atomic interactions leading to growth of clusters and bubbles, but these terms can be easily added. In each equation above, the sums are taken to be infinite, but in a practical sense these terms should be truncated at some finite value. Said in more detail, after the system evolves for some time t , there have been only a finite number of point defects generated and it is unphysical to sum beyond that number. The particular true upper bound of each summation will depend on the generation rate of bubbles and vacancies/interstitials and the consumption rate of these defects in other reactions. Our rationale for using infinite upper bounds is based on the assumptions that (a) the true upper bounds are large and (b) the largest and most important terms in the summation happen well before the upper bound is reached.

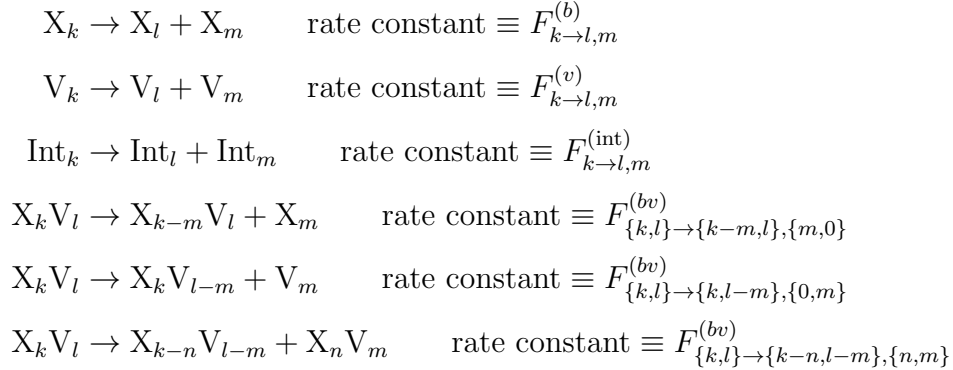
A. Model Details

The system of kinetic equations we use to model point defect evolution is complex both in the number of physical processes that it represents and in the notation needed to identify these reactions. Therefore, in what follows, we give a detailed explanation of the processes involved in the model and then explain what each term in the system of equations represents. There are four species of defect clusters involved in the kinetic model: bubbles (X_k), interstitials (Int_k), voids (V_k), and bubble-void clusters ($X_k V_l$) where each subscript $k, l \in \mathbb{N}$

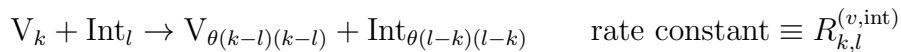
indicates the number of the respective monomeric defects in each cluster. The term denoted by X_k most commonly represents gas bubbles formed through nuclear processes, for example Xe gas in UO_2 or He in Pu. The specific aggregation processes we consider along with the associated rate constants are:



where *aggregation* implies that two species exist on the reactant side of the chemical equation and one species exists on the product side of the equation. The fragmentation reactions we consider along with the associated rate constants are:



where *fragmentation* implies that one species exists on the reactant side of the chemical equation and two species exist on the product side of the equation. In the fragmentation rate constants involving bubble-void clusters, note that the notation $\{m, 0\}$ implies an m -bubble (X_m) and $\{0, m\}$ implies an m -void (V_m). The recombination process included in the model involves voids reacting with interstitials:



where θ is the Heaviside function. We use the term *recombination* to broadly define any reaction in which an interstitial cluster reacts with a void resulting in a reduced number of both species.

Note that all of the processes accounted for in the kinetic model proceed through sequential pathways and we do not include any concerted pathways. For example, we do not account for the reaction in which a 3-cluster fragments into three 1-clusters via a concerted mechanism. In our model, the complete fragmentation of a 3-cluster proceeds sequentially, first by the 3-cluster fragmenting into a 2-cluster and a single interstitial and then by the 2-cluster fragmenting into two interstitials, leaving three interstitial atoms as the final product of the fragmentation reaction.

Equation (1) in the kinetic model,

$$\begin{aligned} \dot{\rho}_1^{(b)} = & G_b(t) - \sum_{i=1}^{\infty} (1 + \delta_{i,1}) A_{i,1}^{(b)} \rho_i^{(b)} \rho_1^{(b)} - \sum_{i=1}^{\infty} A_{i,1}^{(v,b)} \rho_i^{(v)} \rho_1^{(b)} - \sum_{i=1}^{\infty} \sum_{j=1}^{\infty} A_{\{i,j\},1}^{(bv,b)} \rho_{\{i,j\}}^{(bv)} \rho_1^{(b)} \\ & + \sum_{i=2}^{\infty} (1 + \delta_{i-1,1}) F_{i \rightarrow i-1,1}^{(b)} \rho_i^{(b)} + \sum_{i=1}^{\infty} \sum_{j=1}^{\infty} F_{\{i,j\} \rightarrow \{1,0\},\{i-1,j\}}^{(bv)} \rho_{i,j}^{(bv)}, \end{aligned}$$

describes the evolution of the density of monomeric gas, where the first term, $G_b(t)$, is generation rate of gas monomers due to self-irradiation and the second, third, and fourth terms correspond respectively to the loss of density due to: gas monomers combining with gas bubbles of size i to form $(i+1)$ -bubbles, gas monomers combining with i -voids to form $\{1, i\}$ -bubbles, and gas monomers combining with $\{i, j\}$ -bubbles to form $\{i+1, j\}$ -bubbles. The fifth term represents the density increase due to the fragmentation of an i -bubble into a 1-bubble and an $(i-1)$ -bubble. The prefactor term, $1 + \delta_{i-1,1}$, is included to account for the fact that the fragmentation process of a 2-bubble into two monomers increases the monomeric density twofold in comparison to the other fragmentation processes represented in the summation. The sixth term represents the fragmentation of an $\{i, j\}$ -bubble into a $\{1, 0\}$ -bubble (a gas monomer) and an $\{i-1, j\}$ -bubble, i.e., this term represents a gas monomer being ejected by a bubble-void cluster. Equation (2) describes the dynamical evolution of bubbles of size $k \geq 2$:

$$\begin{aligned} \dot{\rho}_k^{(b)} = & - \sum_{i=1}^{\infty} (1 + \delta_{i,k}) A_{i,k}^{(b)} \rho_i^{(b)} \rho_k^{(b)} - \sum_{i=1}^{\infty} A_{i,k}^{(v,b)} \rho_i^{(v)} \rho_k^{(b)} - \sum_{i=1}^{\infty} \sum_{j=1}^{\infty} A_{\{i,j\},k}^{(bv,b)} \rho_{\{i,j\}}^{(bv)} \rho_k^{(b)} \\ & + \frac{1}{2} \sum_{i=1}^{k-1} (1 + \delta_{i,k-i}) A_{i,k-i}^{(b)} \rho_i^{(b)} \rho_{k-i}^{(b)} - \frac{1}{2} \sum_{i=1}^{k-1} (1 + \delta_{i,k-i}) F_{k \rightarrow i,k-i}^{(b)} \rho_k^{(b)} \\ & + \sum_{i=k+1}^{\infty} (1 + \delta_{i-k,k}) F_{i \rightarrow i-k,k}^{(b)} \rho_i^{(b)} + \sum_{i=k}^{\infty} \sum_{j=1}^{\infty} F_{\{i,j\} \rightarrow \{i-k,j\},\{k,0\}}^{(bv)} \rho_{i,j}^{(bv)}, \end{aligned}$$

where the first, second, and third terms correspond to the loss of density due to bubbles of

size k combining with, respectively, bubbles of size i to form a $(k+i)$ -bubbles, voids of size i to form $\{i, k\}$ -bubbles, and bubble-void clusters of size $\{i, j\}$ to form $\{i+k, j\}$ -bubbles. The fourth term corresponds to the formation of a k -bubble due to the aggregation of an i -bubble and a $(k-i)$ -bubble where the factor of $1/2$ is included to avoid overcounting the number of these reactions. The Kronecker delta prefactor is included because when k is an even number the factor $1/2$ is not needed for the $i = k-i$ term in the summation. The fifth term represents the loss of density due to the fragmentation of a k -bubble into an i -bubble and a $(k-i)$ -bubble where the prefactor terms are again included to avoid overcounting. The sixth term corresponds to the density increase due to a bubble of size $i > k$ fragmenting into an $(i-k)$ -bubble and a k -bubble where the prefactor accounts for the doubling needed in the summation to account for the case in which a bubble of size $i = 2k$ fragments into two k -bubbles. The seventh term represents the gain in density due to an $\{i, j\}$ -bubble with $i \geq k$ breaking into an $\{i-k, j\}$ -bubble and k -bubble.

The evolution of voids is described in Eqs. (3) and (4). The third equation,

$$\begin{aligned} \dot{\rho}_1^{(v)} = & G_v(t) - \sum_{i=1}^{\infty} (1 + \delta_{i,1}) A_{i,1}^{(v)} \rho_i^{(v)} \rho_1^{(v)} - \sum_{i=1}^{\infty} A_{1,i}^{(v,b)} \rho_1^{(v)} \rho_i^{(b)} - \sum_{i=1}^{\infty} \sum_{j=1}^{\infty} A_{\{i,j\},1}^{(bv,v)} \rho_{\{i,j\}}^{(bv)} \rho_1^{(v)} \\ & + \sum_{i=2}^{\infty} (1 + \delta_{i-1,1}) F_{i \rightarrow i-1,1}^{(b)} \rho_i^{(v)} + \sum_{i=1}^{\infty} \sum_{j=1}^{\infty} F_{\{i,j\} \rightarrow \{0,1\}, \{i,j-1\}}^{(bv)} \rho_{i,j}^{(bv)} \\ & - \sum_{i=1}^{\infty} R_{1,i}^{(v,int)} \rho_1^{(v)} \rho_i^{(int)} + \sum_{i=2}^{\infty} \sum_{j=i-1}^{\infty} R_{i,j}^{(v,int)} \rho_i^{(v)} \rho_j^{(int)}, \end{aligned}$$

describes the density evolution of single vacancies (1-voids). The first term, $G_v(t)$, is the generation rate of vacancies due to both self-irradiation and thermal effects. The second, third, and fourth terms correspond to the loss of density due to a single vacancy combining with, respectively, voids of size i to form a $(k+i)$ -voids, bubbles of size i to form $\{i, 1\}$ -bubbles, and bubble-void clusters of size $\{i, j\}$ to form $\{i, j+1\}$ -bubbles. The fifth term represents the density increase due to the fragmentation of an i -void into a 1-void and an $(i-1)$ -void where the prefactor term, $1 + \delta_{i-1,1}$, is included to account for the fact that the process of a 2-void fragmenting into two monomers increases the density of single vacancies twofold in comparison to the other terms in the summation. The sixth term represents the fragmentation of an $\{i, j\}$ -bubble into a $\{0, 1\}$ -bubble (a vacancy) and an $\{i, j-1\}$ -bubble. The seventh term represents the loss of density due to the recombination of a single vacancy and a cluster of size i (leaving a cluster of size $i-1$) and the eighth term represents the

density increase due to the recombination of an void of size $i \geq 2$ and a $(i-1)$ -cluster leaving a single vacancy. Equation 4,

$$\begin{aligned}
\dot{\rho}_k^{(v)} = & - \sum_{i=1}^{\infty} (1 + \delta_{i,k}) A_{i,k}^{(v)} \rho_i^{(v)} \rho_k^{(v)} - \sum_{i=1}^{\infty} A_{k,i}^{(v,b)} \rho_k^{(v)} \rho_i^{(b)} - \sum_{i=1}^{\infty} \sum_{j=1}^{\infty} A_{\{i,j\},k}^{(bv,v)} \rho_{\{i,j\}}^{(bv)} \rho_k^{(v)} \\
& + \frac{1}{2} \sum_{i=1}^{k-1} (1 + \delta_{i,k-i}) A_{i,k-i}^{(v)} \rho_i^{(v)} \rho_{k-i}^{(v)} - \frac{1}{2} \sum_{i=1}^{k-1} (1 + \delta_{i,k-i}) F_{k \rightarrow i,k-i}^{(v)} \rho_k^{(v)} \\
& + \sum_{i=k+1}^{\infty} (1 + \delta_{i-k,k}) F_{i \rightarrow i-k,k}^{(v)} \rho_i^{(v)} + \sum_{i=1}^{\infty} \sum_{j=k}^{\infty} F_{\{i,j\} \rightarrow \{i,j-k\},\{0,k\}}^{(bv)} \rho_{i,j}^{(bv)} \\
& - \sum_{i=1}^{\infty} R_{k,i}^{(v,int)} \rho_k^{(v)} \rho_i^{(int)} + \sum_{i=k+1}^{\infty} \sum_{j=i-1}^{\infty} R_{i,j}^{(v,int)} \rho_i^{(v)} \rho_j^{(int)},
\end{aligned}$$

describes the evolution of k -voids for $k \geq 2$. The first, second, and third terms correspond to the loss of density due to voids of size k combining with, respectively, voids of size i to form a $(k+i)$ -voids, bubbles of size i to form $\{i, k\}$ -bubbles, and bubble-void clusters of size $\{i, j\}$ to form $\{i, j+k\}$ -bubbles. The fourth term corresponds to the formation of a k -void due to the aggregation of an i -void and a $(k-i)$ -void. The fifth term represents the loss of density due to the fragmentation of a k -void into an i -void and a $(k-i)$ -void. The sixth and seventh terms correspond to the density increases due to, respectively, a void of size $i > k$ fragmenting into an $(i-k)$ -void and a k -void and a $\{i, j\}$ -bubble with $j \geq k$ fragmenting into an $\{i, j-k\}$ -bubble and k -void. The eighth term represents the loss of density due to the recombination of a k -void and a cluster of size i and the ninth term represents the density increase due to the recombination of an void of size $k+i$ and a i -cluster leaving a k -void.

The fifth equation:

$$\begin{aligned}
\dot{\rho}_{\{k,l\}}^{(bv)} = & - \sum_{i=1}^{\infty} A_{\{k,l\},i}^{(bv,b)} \rho_{\{k,l\}}^{(bv)} \rho_i^{(b)} - \sum_{i=1}^{\infty} A_{\{k,l\},i}^{(bv,v)} \rho_{\{k,l\}}^{(bv)} \rho_i^{(v)} \\
& - \sum_{i=1}^{\infty} \sum_{j=1}^{\infty} (1 + \delta_{\{k,l\},\{i,j\}}) A_{\{k,l\},\{i,j\}}^{(bv)} \rho_{\{k,l\}}^{(bv)} \rho_{\{i,j\}}^{(bv)} + \sum_{i=1}^{k-1} A_{\{k-i,l\},i}^{(bv,b)} \rho_{\{k-i,l\}}^{(bv)} \rho_i^{(b)} \\
& + \sum_{i=1}^{l-1} A_{\{k,l-i\},i}^{(bv,v)} \rho_{\{k,l-i\}}^{(bv)} \rho_i^{(v)} + A_{k,l}^{(b,v)} \rho_k^{(b)} \rho_l^{(v)} + \sum_{i=1}^{k-1} \sum_{j=1}^{l-1} A_{\{k-i,l-j\},\{i,j\}}^{(bv)} \rho_{\{k-i,l-j\}}^{(bv)} \rho_{\{i,j\}}^{(bv)} \\
& - \sum_{i=1}^k \left(1 - \frac{\delta_{k-i,0}}{2}\right) F_{\{k,l\} \rightarrow \{k-i,l\},\{i,0\}}^{(bv)} \rho_{\{k,l\}}^{(bv)} - \sum_{i=1}^l \left(1 - \frac{\delta_{l-i,0}}{2}\right) F_{\{k,l\} \rightarrow \{k,l-i\},\{0,i\}}^{(bv)} \rho_{\{k,l\}}^{(bv)} \\
& - \sum_{i=1}^{k-1} \sum_{i=1}^{l-1} F_{\{k,l\} \rightarrow \{k-i,l-j\},\{i,j\}}^{(bv)} \rho_{\{k,l\}}^{(bv)} + \sum_{i=1}^{\infty} F_{\{k+i,l\} \rightarrow \{k,l\},\{i,0\}}^{(bv)} \rho_{\{k+i,l\}}^{(bv)} \\
& + \sum_{i=1}^{\infty} F_{\{k,l+i\} \rightarrow \{k,l\},\{0,i\}}^{(bv)} \rho_{\{k,l+i\}}^{(bv)} + \sum_{i=1}^{\infty} \sum_{j=1}^{\infty} F_{\{k+i,l+j\} \rightarrow \{k,l\},\{i,j\}}^{(bv)} \rho_{\{k+i,l+j\}}^{(bv)},
\end{aligned}$$

describes the evolution of bubble-void clusters. The first, second, and third terms correspond to the loss of density due to $\{k, l\}$ -bubbles combining with, respectively, bubbles of size i , voids of size i , and bubble-void clusters of size $\{i, j\}$. The fourth and fifth terms correspond respectively to the density increases generated by $\{k - i, l\}$ -bubbles aggregating with i -bubbles and $\{k, l - i\}$ -bubbles aggregating with i -voids. The sixth term represents the density increase due to a k -bubble combining with an l -void to form a $\{k, l\}$ -bubble. The seventh term accounts for bubbles of size $\{k - i, l - j\}$ combining with bubbles of size $\{i, j\}$ to form $\{k, l\}$ -bubbles. The eighth term corresponds to $\{k, l\}$ -bubbles fragmenting into $\{k - i, l\}$ -bubbles and i -bubbles and the ninth term corresponds to $\{k, l\}$ -bubbles fragmenting into $\{k, l - i\}$ -bubbles and i -voids where the prefactors in these two terms eliminate overcounting the product $\{0, l\}, \{k, 0\}$ in eighth term and the product $\{k, 0\}, \{0, l\}$ in the ninth term, which are the same product. The tenth term represents the density loss due to a bubble of size $\{k, l\}$ fragmenting into bubbles of size $\{k - i, l - j\}$ and $\{i, j\}$. The eleventh, twelfth, and thirteenth terms respectively represent density increases due to the fragmentation of: $\{k + i, l\}$ -bubbles into $\{k, l\}$ -bubbles and $\{i, 0\}$ -bubbles, $\{k, l + i\}$ -bubbles into $\{k, l\}$ -bubbles and $\{0, i\}$ -bubbles, and $\{k + i, l + j\}$ -bubbles into $\{k, l\}$ -bubbles and $\{i, j\}$ -bubbles.

The last two equations represent the time evolution of interstitials. Equation (6),

$$\begin{aligned} \dot{\rho}_1^{(\text{int})} = & G_{\text{int}}(t) - \sum_{i=1}^{\infty} (1 + \delta_{i,1}) A_{i,1}^{(\text{int})} \rho_i^{(\text{int})} \rho_1^{(\text{int})} + \sum_{i=2}^{\infty} (1 + \delta_{i-1,1}) F_{i \rightarrow i-1,1}^{(\text{int})} \rho_i^{(\text{int})} \\ & - \sum_{i=1}^{\infty} R_{i,1}^{(v,\text{int})} \rho_i^{(v)} \rho_1^{(\text{int})} + \sum_{i=2}^{\infty} \sum_{j=i-1}^{\infty} R_{j,i}^{(v,\text{int})} \rho_j^{(v)} \rho_i^{(\text{int})}, \end{aligned}$$

describes the growth rate of the density of monomeric interstitial atoms. The first term, $G_{\text{int}}(t)$, is generation rate of interstitials due to self-irradiation and thermal effects. The second term represents the loss of density of interstitials due to the aggregation of interstitial clusters of size i and size 1 to form $(i+1)$ -clusters. The third term represents the density increase due to the fragmentation of a i -cluster into a 1-cluster and an $(i-1)$ -cluster where the prefactor, $1 + \delta_{i-1,1}$, is included to account for the fact that the fragmentation process of a 2-cluster into two interstitials increases the monomeric density twofold in comparison to the other processes. The fourth term represents the loss of density due to the recombination of a monomeric interstitial and a void of size i (leaving a void of size $i-1$) and the fifth term represents the density increase due to the recombination of an interstitial cluster of size $i \geq 2$ and a $(i-1)$ -void leaving a single interstitial. Note that we assume that there is no multiple occupancy of a vacancy by an interstitial in the recombination process. The final equation in the kinetic model:

$$\begin{aligned} \dot{\rho}_k^{(\text{int})} = & - \sum_{i=1}^{\infty} (1 + \delta_{i,k}) A_{i,k}^{(\text{int})} \rho_i^{(\text{int})} \rho_k^{(\text{int})} + \frac{1}{2} \sum_{i=1}^{k-1} (1 + \delta_{i,k-i}) A_{i,k-i}^{(\text{int})} \rho_i^{(\text{int})} \rho_{k-i}^{(\text{int})} \\ & - \frac{1}{2} \sum_{i=1}^{k-1} (1 + \delta_{k-i,i}) F_{k \rightarrow k-i,i}^{(\text{int})} \rho_k^{(\text{int})} + \sum_{i=k+1}^{\infty} (1 + \delta_{i-k,k}) F_{i \rightarrow i-k,k}^{(\text{int})} \rho_i^{(\text{int})} \\ & - \sum_{i=1}^{\infty} R_{i,k}^{(v,\text{int})} \rho_i^{(v)} \rho_k^{(\text{int})} + \sum_{i=k+1}^{\infty} \sum_{j=i-1}^{\infty} R_{j,i}^{(v,\text{int})} \rho_j^{(v)} \rho_i^{(\text{int})}, \end{aligned}$$

describes the growth rate of the density of clusters of $k \geq 2$ interstitial atoms. The first term corresponds the loss of density due to clusters of size k combining with clusters of size i to form a $(k+i)$ -cluster and the second term corresponds to the formation of a k -cluster due to the aggregation of an i -cluster and a $(k-i)$ -cluster. In the second term, the factor of $1/2$ prevents overcounting, meaning that aggregation of i and $k-i$ clusters and $k-i$ and i clusters represent the same process. The prefactor, $1 + \delta_{i,k-i}$, accounts for the fact that the factor $1/2$ is not needed in the $i = k-i$ term in the summation when k is even. The third term represents the loss of density due to the fragmentation of a k -cluster into an i -cluster

and a $(k - i)$ -cluster where the prefactor terms are included to avoid overcounting. The fourth term corresponds to the density increase due to a cluster of size $i > k$ fragmenting into an $(i - k)$ -cluster and a k -cluster where the prefactor accounts for the doubling needed in the summation to account for the case in which a cluster of size $i = 2k$ fragments into two k -clusters. The fifth term represents the loss of density due to the recombination of a k -cluster and a void of size i and the sixth term represents the density increase due to the recombination of an interstitial cluster of size $k + i$ and a i -void leaving a k -cluster.

III. RATE CONSTANTS

The system of kinetic equations defined in Sec. II above is given in a generalized form that can be broadly applied to understand point and volume defect evolution in irradiated materials. The generalized system of equations becomes specific to a particular material through the assignment and evaluation of values for the rate constants and defect generation rates. In this Section, we derive functional forms for the aggregation, recombination, and fragmentation rate constants. Two principal assumptions are used in the derivations: (a) the material is in a thermal equilibrium and can be defined by a global time-independent temperature and (b) the reaction dynamics in the material follow Arrhenius kinetics. More specifically, we use assumptions based on transition state theory^{26,28} and classical nucleation theory²⁷ in order to derive functional forms for each rate constant.

A. Aggregation

Each aggregation process involves two reactants combining to form a single product cluster. Here, we assume that the geometry of defect clusters can be well-described using a spherical approximation. In this approximation, the rate constant for an aggregation reaction between an i -sized cluster of species $s \in \{b, v, bv, \text{int}\}$ and a j -sized cluster of species $s' \in \{b, v, bv, \text{int}\}$ (excluding combinations involving voids and interstitials as well as bubbles and interstitials) can be defined as

$$A_{i,j}^{(s,s')} = 4\pi r_{i,j}^{(s,s')} D_{i,j}^{(s,s')} \kappa_{i,j}^{(s,s')} \exp\left[-\frac{E_{i,j}^{(s,s')}}{k_B T}\right], \quad (8)$$

where

$$r_{i,j}^{(s,s')} = r_i^{(s)} + r_j^{(s')}, \quad (9)$$

is the capture radius between the aggregating reactants with $r_i^{(s)}$ and $r_j^{(s')}$ being the effective radii of the i - and j -sized clusters of species s and s' . The effective diffusion coefficient

$$D_{i,j}^{(s,s')} = D_i^{(s)} + D_j^{(s')}, \quad (10)$$

characterizes the Brownian motion of the species s sphere relative to the center of the sphere of species s' , which is itself also undergoing Brownian motion,²⁹ where $D_i^{(s)}$ and $D_j^{(s')}$ are respectively the diffusion coefficients of the i - and j -sized clusters of species s and s' . The factor $\kappa_{i,j}^{(s,s')}$ is the standard transmission coefficient from transition state theory (TST) that characterizes the probability that a collision event between spheres that has energy above the activation energy proceeds to form a product. The limit $\kappa_{i,j}^{(s,s')} = 1$ implies that all collisions with energy above $E_{i,j}^{(s,s')}$ go on to the product state. This factor can be interpreted as accounting for the true geometric effects of the reacting clusters, i.e., nonspherical cluster geometries. For notational convenience, if $s' = s$ (meaning that only a single species is involved in the reaction) then $A_{i,j}^{(s,s')}$, $D_{i,j}^{(s,s')}$, and $r_{i,j}^{(s,s')}$ are respectively written as $A_{i,j}^{(s)}$, $D_{i,j}^{(s)}$, and $r_{i,j}^{(s)}$. We assume that the diffusion processes for the two reactants are independent and therefore the effective diffusion coefficient is given by the sum of diffusion coefficients for each species. The Boltzmann factor $e^{-E_{i,j}^{(s,s')}/k_{\text{B}}T}$ in Eq. (8) represents the probability that two colliding clusters will combine, where $E_{i,j}^{(s,s')}$ is the activation energy, sometimes called the attachment barrier, for the aggregation process. The temperature dependence of the diffusion coefficient for an i -sized cluster of species s is commonly accounted for using the expression

$$D_i^{(s)} = \bar{D}_i^{(s)} \exp \left[-\frac{E_{\text{m}_i}^{(s)}}{k_{\text{B}}T} \right], \quad (11)$$

where $E_{\text{m}_i}^{(s)}$ is the migration energy. Equation (8) can be interpreted using the Arrhenius picture of reaction kinetics as the frequency that reactant spheres contact each other multiplied by the probability that a contact event leads to the two spheres aggregating. Details of the rate constant derivation in the activationless $E_{i,j}^{(s,s')} = 0$ regime can be found in Refs. 29 and 30. Note that the activationless regime is widely used in the literature to describe aggregation processes in irradiated materials and implies that two colliding clusters combine with unit probability.

The volume of a species s cluster of size n is $V_n^{(s)} = nV_1^{(s)}$ where $V_1^{(s)}$ is the volume of a single (point) defect of that species. For bubbles ($s = b$) and interstitials ($s = \text{int}$), the single defect volume is respectively the atomic volume of a single gas atom and the volume of a single atom of the base material. In the case of voids ($s = v$), $V_1^{(s)}$ is the effective volume of a single vacancy. Using the spherical cluster approximation implies that the effective radius for an n -sized cluster of species $s \in \{b, v, \text{int}\}$ is³¹

$$r_n^{(s)} = \left(\frac{3nV_1^{(s)}}{4\pi} \right)^{1/3} = r_1^{(s)} n^{1/3}. \quad (12)$$

For bubble-void clusters, the situation is more complex because gas atoms in the cluster can take two configurations: interstitial and substitutional, where the interstitial atoms contribute to the volume of the cluster while the substitutional atoms do not. First, we define the volume of a bubble-void cluster of size $n = \{i, j\}$ as

$$V_n^{(s)} = V_{wi}^{(b)} + V_j^{(v)}, \quad (13)$$

where $V_j^{(v)}$ is the volume of a void of size j and $V_{wi}^{(b)}$ is the volume taken up by the i gas atoms in the cluster with w being the fraction of gas atoms that are interstitials. This implies that the effective radius of bubble-void clusters is

$$r_n^{(s)} = \left(\frac{3V_n^{(s)}}{4\pi} \right)^{1/3}, \quad (14)$$

where $V_n^{(s)}$ is defined in Eq. (13). When all the gas atoms in the cluster are substitutional $w = 0$ and when all the gas atoms are interstitial $w = 1$; mixtures of interstitial and substitutional gas atoms will lead to different values for w . Using a mean field approximation, w can be defined as the average fraction of interstitial gas atoms in the bubble-void clusters: $w = \langle w \rangle$. This approximation leads to the definition: $V_n^{(s)} = V_{\langle w \rangle i}^{(b)} + V_j^{(v)}$.

In summary, the practical evaluation of aggregation rate constants requires information about: (a) the diffusion coefficients of each species involved in the reaction, (b) the volumes of the different defects which are used to evaluate the capture radius for the reaction, and (c) the attachment energies.

Formally, the diffusion coefficient of each species depends on the structural configuration of the material, which changes as the irradiation and/or self-irradiation processes proceed. To account for these changes in the above formalism, we define a reaction progress variable

$\lambda \in [0, 1]$ that parameterizes the extent of the reaction as a function of time t , where $\lambda = 0$ denotes the material in an unradiated state at $t = 0$ and $\lambda = 1$ is the steady-state $t \rightarrow \infty$ limit where the concentration of each defect species is not changing in time. In this time-dependent picture that accounts for structural modifications in the material, the rate constant can be recast as:

$$A_{i,j}^{(s,s')}(\lambda) = 4\pi \left(r_i^{(s)} + r_j^{(s')} \right) \left(D_i^{(s)}(\lambda) + D_j^{(s')}(\lambda) \right) \kappa_{i,j}^{(s,s')}(\lambda) \exp \left[-\frac{E_{i,j}^{(s,s')}}{k_B T} \right]. \quad (15)$$

where the diffusion coefficients now depend on λ . Practically speaking, due to the complexity of calculating time-dependent properties, it will almost always be advantageous to first assume that the rate constants can be well-described as time-independent and then to modify this assumption as needed based on empirical evidence gained by comparing theoretical results with experimental observations. This problem may be mitigated using data-driven and machine learning approaches which may be better able to determine system parameters, specifically time-dependent properties.^{32–37}

B. Recombination

Recombination reactions occur between voids (clusters of vacancies) and clusters of interstitial atoms of the base material. The recombination process considered here involves two steps: First, the interstitial atoms in the cluster occupy the vacancies in the void and, second, the larger of the two reactant species fragments. This means that the result of a recombination reaction is the filling or partial filling of the void and, if the reactant cluster and void are not the same size, a smaller void or cluster that arises through fragmentation. Applying similar physics as those used to derive the aggregation rate constant, the recombination rate between voids of size i and interstitial clusters of size j is

$$R_{i,j}^{(v,int)} = 4\pi r_{i,j}^{(v,int)} D_{i,j}^{(v,int)} \kappa_{i,j}^{(v,int)} \exp \left[-\frac{E_{i,j}^{(v,int)}}{k_B T} \right] \exp \left[-\frac{G_{k \rightarrow l, |i-j|}^{(s)}}{k_B T} \right], \quad (16)$$

where $E_{i,j}^{(v,int)}$ is the activation energy for the recombination process and $G_{k \rightarrow l, |i-j|}^{(s)}$ is the activation energy for fragmentation of the larger (by number of monomeric constituents) species in the reaction with $s = v$, $k = i$, $l = j$ if $i > j$ and $s = \text{int}$, $k = j$, $l = i$ if $i < j$. The other parameters in Eq. (16) are defined in the same way as in Eq. (8). In the case

that the void is larger than the interstitial cluster ($i > j$) the recombination process leaves a void of size $|i - j|$ and when the cluster is larger than the void ($j > i$) a cluster of size $|i - j|$ remains after the recombination. In the case $i = j$, there is no fragmentation and the fragmentation energy is zero.

Assuming the recombination and corresponding fragmentation processes are independent allows us to write the process probability as a product of each of the individual probabilities as represented by the exponential terms in Eq. (16) above. Because we have assumed that the capture and fragmentation steps in the reaction are independent, the rate constant can be interpreted as the frequency that i -voids and j -clusters come into contact multiplied by (a) the probability that each contact leads to a successful recombination and (b) the probability that the energy of the primary activated complex in the reaction also has sufficient energy to surmount the fragmentation activation barrier leading to the proper fragmentation product. Here, the primary activated complex is taken to occur when the the atoms in the cluster have filled the void but the fragmentation of either the void or cluster (whichever is larger) has not yet occurred.

In order to evaluate the recombination rate we need information about the diffusion characteristics of the voids and clusters, the point defect volume and the activation energy of the aggregation and energy fragmentation processes. Also, in a similar fashion to what was done for the aggregation rate constants, the recombination rate can be modified to treat structural changes in the material that arise as the irradiation process proceeds by defining the diffusion coefficients to depend on the reaction progress variable λ .

C. Fragmentation

We consider cluster fragmentation processes that can be induced by either thermal fluctuations or by a collision between clusters. The functional form we use for the fragmentation rate constant is

$$F_{i \rightarrow j,k}^{(s)} = \kappa_{i \rightarrow j,k}^{(s)} \frac{A_{j,k}^{(s)}}{V_i^{(s)}} \exp \left[-\frac{E_{b_{i \rightarrow j,k}}^{(s)}}{k_B T} \right], \quad (17)$$

where $A_{j,k}^{(s)}$ is the rate constant for the reverse aggregation process (the cluster formation) and $E_{b_{i \rightarrow j,k}}^{(s)}$ is a binding energy that characterizes the energy difference between the reactant i -sized cluster and the product fragments of size j and size k . Note that the binding energy is

the energy difference between the stable reactant and product states and is not an activation energy. The other parameters are defined as in Eq. (8). Also note that the transmission coefficient for fragmentation process may not be equal to the transmission coefficient for the reverse aggregation process, i.e., it is not rigorously true that $\kappa_{i \rightarrow j,k}^{(s)} = \kappa_{j,k}^{(s)}$. Equation 17 arises from a detailed balance assumption, and in the $\kappa_{i \rightarrow j,k}^{(s)} \rightarrow 1$ limit is the same rate constant as that used by Stewart *et al.* in Ref. 25.

The above picture of the fragmentation rate constant is advantageous from a practical implementation perspective because once the aggregation rate is known, evaluating the corresponding fragmentation rate only requires information about the binding energy and the transmission coefficient. However, this reaction picture does not account for the multiple reaction pathways, and different dynamics along these pathways, that can lead from an i -sized cluster to j - and k -sized fragments. For example, the rate of ejection of a dimer from the center of the cluster will be much slower than the rate of ejection of a dimer from the surface of the cluster, and the difference between these two rates is not accounted for in Eq. (17). Accounting for each possible $i \rightarrow j,k$ pathway is a complicated combinatorial problem and it will often be impractical to evaluate the dynamics along each pathway. Therefore, the number fragmentation processes are often simplified by assuming that only monomers can be ejected from a cluster, i.e, that the only possible fragmentation process is $i \rightarrow 1, i - 1$.

IV. CONCLUSIONS

We have introduced a generalized theoretical framework to describe point and volume defect evolution in irradiated materials. In order to apply this framework to a specific material, the defect generation rates and the parameters contained in the rate constants must be assigned. In general, these parameters will come from experimental observations, electronic structure calculations, and/or atomistic simulations.

While we have derived the kinetic equations using a picture that accounts for the mobility of clusters of all sizes, it may often be advantageous to simplify the equations in order to make them computationally tractable and more physical meaningful. For example, it is known that the mobility of clusters will typically decrease with increasing cluster size, and, as clusters grow large, the diffusional timescale is such that the timescale of the overall

chemical process is much faster. This implies that it is often not only reasonable to ignore the mobility of large clusters, but, from a practical perspective, it is essential in order to reduce the complexity of the system of equations.

The thermodynamics and kinetics in the model are described using equilibrium assumptions, however, it is known that sequential assembly^{38–45} and more broadly nonequilibrium assembly processes⁴⁶ result in structures and cluster geometries that can vary significantly from the equilibrium results. It may be advantageous in the modeling of some systems to consider the role and extent that nonequilibrium assembly plays on the kinetics and cluster distribution. The developed theory could also be modified to rigorously treat systems that are dominated by nonspherical cluster geometries and therefore nonspherical diffusion properties. More specifically, the treatment of nonspherical cluster geometries will be required when two-dimensional defects (for example, dislocation lines and loops) play a prominent role in the macroscopic structural changes in the material.

V. ACKNOWLEDGMENTS

This work was supported by the U.S. Department of Energy through Los Alamos National Laboratory (LANL).

* gcraven@lanl.gov

† bwilson@lanl.gov

¹ G. S. Was, *Fundamentals of Radiation Materials Science: Metals and Alloys* (Springer, 2016).

² H. Trinkaus and B. Singh, *J. Nucl. Mater.* **323**, 229 (2003), doi:10.1016/j.jnucmat.2003.09.001.

³ C. J. Ortiz and M. J. Caturla, *Phys. Rev. B* **75**, 184101 (2007), doi:10.1103/PhysRevB.75.184101.

⁴ M. P. Surh, J. B. Sturgeon, and W. G. Wolfer, *J. Nucl. Mater.* **378**, 86 (2008), doi:10.1016/j.jnucmat.2008.05.009.

⁵ B. D. Wirth, X. Hu, A. Kohnert, and D. Xu, *J. Mater. Res.* **30**, 1440–1455 (2015), doi:10.1557/jmr.2015.25.

- ⁶ A. A. Kohnert, B. D. Wirth, and L. Capolungo, *Compl. Matls. Sci.* **149**, 442 (2018), doi:10.1016/j.commatsci.2018.02.049.
- ⁷ A. J. Schwartz, M. A. Wall, T. G. Zocco, and W. G. Wolfer, *Philos. Mag.* **85**, 479 (2005), doi:10.1080/02678370412331320026.
- ⁸ S. I. Golubov, A. M. Ovcharenko, A. V. Barashev, and B. N. Singh, *Philos. Mag. A* **81**, 643 (2001), doi:10.1080/01418610108212164.
- ⁹ M. F. Wehner and W. G. Wolfer, *Philos. Mag. A* **52**, 189 (1985), doi:10.1080/01418618508237618.
- ¹⁰ R. Singleton, D. Preston, and B. Wilson, Tech. Rep., Los Alamos National Laboratory (2019).
- ¹¹ L. Bonilla, A. Carpio, J. Neu, and W. Wolfer, *Physica D* **222**, 131 (2006), doi:10.1016/j.physd.2006.07.029.
- ¹² X. Gai, T. Lazauskas, R. Smith, and S. D. Kenny, *J. Nucl. Mater.* **462**, 382 (2015), doi:10.1016/j.jnucmat.2014.10.027.
- ¹³ S.-H. Li, J.-T. Li, and W.-Z. Han, *Materials* **12**, 1036 (2019), doi:10.3390/ma12071036.
- ¹⁴ C. Schaldach and W. Wolfer, in *Effects of Radiation on Materials: 21st International Symposium* (ASTM International, 2004).
- ¹⁵ C. Thiebaut, N. Baclet, B. Ravat, P. Giraud, and P. Julia, *J. Nucl. Mater.* **361**, 184 (2007), doi:10.1016/j.jnucmat.2006.12.024.
- ¹⁶ S. Sharafat, A. Takahashi, K. Nagasawa, and N. Ghoniem, *J. Nucl. Mater.* **389**, 203 (2009), doi:10.1016/j.jnucmat.2009.02.027.
- ¹⁷ D. Xu and B. D. Wirth, *Fusion. Sci. Technol.* **56**, 1064 (2009), doi:10.13182/FST09-A9052.
- ¹⁸ J. Jeffries, M. Wall, K. Moore, and A. Schwartz, *J. Nucl. Mater.* **410**, 84 (2011), doi:10.1016/j.jnucmat.2011.01.015.
- ¹⁹ J. Jeffries, J. Hammons, T. Willey, M. Wall, D. Ruddle, J. Ilavsky, P. Allen, and T. van Buuren, *J. Nucl. Mater.* **498**, 505 (2018), doi:10.1016/j.jnucmat.2017.10.058.
- ²⁰ D. Xu, X. Hu, and B. D. Wirth, *Appl. Phys. Lett.* **102**, 011904 (2013), doi:10.1063/1.4773876.
- ²¹ M. A. Tschopp, F. Gao, L. Yang, and K. N. Solanki, *J. Appl. Phys.* **115**, 033503 (2014), doi:10.1063/1.4861719.
- ²² C. Wang, C. Ren, W. Zhang, H. Gong, P. Huai, Z. Zhu, H. Deng, and W. Hu, *Compl. Matls. Sci.* **107**, 54 (2015), doi:10.1016/j.commatsci.2015.05.017.

- ²³ C. Matthews, R. Perriot, M. W. Cooper, C. R. Stanek, and D. A. Andersson, *J. Nucl. Mater.* **527**, 151787 (2019), doi:10.1016/j.jnucmat.2019.151787.
- ²⁴ C. Matthews, R. Perriot, M. Cooper, C. R. Stanek, and D. A. Andersson, *J. Nucl. Mater.* **540**, 152326 (2020), doi:10.1016/j.jnucmat.2020.152326.
- ²⁵ J. A. Stewart, A. A. Kohnert, L. Capolungo, and R. Dingreville, *Compl. Matls. Sci.* **148**, 272 (2018), doi:10.1016/j.commatsci.2018.02.048.
- ²⁶ D. G. Truhlar, B. C. Garrett, and S. J. Klippenstein, *J. Phys. Chem.* **100**, 12771 (1996), doi:10.1021/jp953748q.
- ²⁷ K. C. Russell, *Metall. Mater. Trans. A* **39**, 956 (2008), doi:10.1007/s11661-007-9352-x.
- ²⁸ G. T. Craven and R. Hernandez, *Phys. Rev. Lett.* **115**, 148301 (2015), doi:10.1103/PhysRevLett.115.148301.
- ²⁹ A. Philipse, *Notes on Brownian Motion* (2011).
- ³⁰ M. Von Smoluchowski, *Tech. Rep.*, Army Biological Labs (1968).
- ³¹ C. Dethloff, E. Gaganidze, V. V. Svetukhin, and J. Aktaa, *J. Nucl. Mater.* **426**, 287 (2012), ISSN 0022-3115, doi:10.1016/j.jnucmat.2011.12.025.
- ³² N. Lubbers, J. S. Smith, and K. Barros, *J. Chem. Phys.* **148**, 241715 (2018), doi:10.1063/1.5011181.
- ³³ P. L. Houston, A. Nandi, and J. M. Bowman, *J. Phys. Chem. Lett.* **10**, 5250 (2019), doi:10.1021/acs.jpcllett.9b01810.
- ³⁴ A. Nandi, J. M. Bowman, and P. Houston, *J. Phys. Chem. A* **124**, 5746 (2020), doi:10.1021/acs.jpca.0c04348.
- ³⁵ G. T. Craven, N. Lubbers, K. Barros, and S. Tretiak, *J. Phys. Chem. Lett.* **11**, 4372–4378 (2020), doi:10.1021/acs.jpcllett.0c00627.
- ³⁶ G. T. Craven, N. Lubbers, K. Barros, and S. Tretiak, *J. Chem. Phys.* **153**, 104502 (2020), doi:10.1063/5.0017894.
- ³⁷ E. Komp and S. Valteau, *J. Phys. Chem. A* **124**, 8607 (2020), doi:10.1021/acs.jpca.0c05992.
- ³⁸ B. Widom, *J. Chem. Phys.* **44**, 3888 (1966), doi:10.1063/1.1726548.
- ³⁹ J. Feder, *J. Theor. Biol.* **87**, 237 (1980), doi:10.1016/0022-5193(80)90358-6.
- ⁴⁰ S. L. James, *Chem. Soc. Rev.* **32**, 276 (2003), doi:10.1039/B200393G.
- ⁴¹ S. Torquato, O. U. Uche, and F. H. Stillinger, *Phys. Rev. E* **74**, 061308 (2006), doi:10.1103/PhysRevE.74.061308.

- ⁴² M. Cieřła, *J. Stat. Mech.* **2013**, P07011 (2013), doi:10.1088/1742-5468/2013/07/P07011.
- ⁴³ M. Cieřła and P. Karbowniczek, *Phys. Rev. E* **91**, 042404 (2015), doi:10.1103/PhysRevE.91.042404.
- ⁴⁴ G. T. Craven, A. V. Popov, and R. Hernandez, *J. Phys. Chem. B* **118**, 14092 (2014), doi:10.1021/jp505207h.
- ⁴⁵ Y. Zhang, A. McMullen, L.-L. Pontani, X. He, R. Sha, N. C. Seeman, J. Brujic, and P. M. Chaikin, *Nat. Commun.* **8**, 1 (2017).
- ⁴⁶ M. Nguyen and S. Vaikuntanathan, *Proc. Natl. Acad. Sci.* **113**, 14231 (2016), doi:10.1073/pnas.1609983113.